CLINICAL ORAL IMPLANTS RESEARCH

Sun-Young Lee
Dong-Jun Yang
Shinil Yeo
Hyun-Wook An
Kyung Ho Ryoo
Kwang-Bum Park

The cytocompatibility and osseointegration of the Ti implants with XPEED® surfaces

Authors' affiliations:
Sun-Young Lee, Dong-Jun Yang, Shinil Yeo, Hyun-Wook An, Kyung Ho Ryoo, Kwang-Bum Park, Department of Biobusiness, Megagen Implant, Gyeongsan si, Gyeongsangbuk-do, South Korea

Corresponding author:
Kwang-Bum Park MD
Megagen Implant
Gyochon-ri, Jain-myeon
Gyeongsan si
Gyeongsangbuk-do 712-852
South Korea
Tel.: +82 2 070 7115 0900
Fax: +82 53 857 5774
e-mail: periopkb@hanmail.net

Key words: calcium, cytocompatibility, incorporation, osseointegration, surface treatment, titanium implant, XPEED®

Abstract

Objectives: This study evaluated cytocompatibility and osseointegration of the titanium (Ti) implants with resorbable blast media (RBM) surfaces produced by grit-blasting or XPEED® surfaces by coating of the nanostructured calcium.

Material and methods: Ti implants with XPEED® surfaces were hydrothermally prepared from Ti implants with RBM surfaces in a solution containing alkaline calcium. The surface characteristics were evaluated by using a scanning electron microscope (SEM) and surface roughness measuring system. Apatite formation was measured with SEM after immersion in modified-simulated body fluid and the amount of calcium released was measured by inductively coupled plasma optical emission. The cell proliferation was investigated by MTT assay and the cell attachment was evaluated by SEM in MC3T3-E1 pre-osteoblast cells. Thirty implants with RBM surfaces and 30 implants with XPEED® surfaces were placed in the proximal tibiae and in the femoral condyles of 10 New Zealand White rabbits. The osseointegration was evaluated by a removal torque test in the proximal tibiae and by histomorphometric analysis in the femoral condyles 4 weeks after implantation.

Results: The Ti implants with XPEED® surfaces showed a similar surface morphology and surface roughness to those of the Ti implants with RBM surfaces. The amount of calcium ions released from the surface of the Ti implants with XPEED® surfaces was much more than the Ti implants with RBM surfaces ($P < 0.05$). The cell proliferation and cell attachment of the Ti implants showed a similar pattern to those of the Ti implants with RBM surfaces ($P > 0.1$). Apatite deposition significantly increased in all surfaces of the Ti implants with XPEED® surfaces. The removable torque value ($P = 0.038$) and percentage of bone-to-implant contact (BIC%) ($P = 0.03$) was enhanced in the Ti implants with XPEED® surfaces.

Conclusion: The Ti implants with XPEED® surfaces significantly enhanced apatite formation, removal torque value, and the BIC%. The Ti implants with XPEED® surfaces may induce strong bone integration by improving osseointegration of grit-blasted Ti implants in areas of poor quality bone.

Surface roughness and topography is a crucial factor for osseointegration and the biomechanical stability of dental implants. Surface roughness is classified into three different surface types, macro-sized, micro-sized, and nano-sized topography. The range of macro-sized roughness is more than 10 μm and is associated with threaded screw and macroporous surfaces produced by macroporous surface treatments. This macro scale is associated with implant geometry. Various studies have reported that surfaces with macro-sized roughness are superior to smooth surfaces at the time of early fixation and mechanical stability (Buser et al. 1991; Gotfredsen et al. 1995; Wennerberg et al. 1995). The range of micro-sized roughness made by common surface treatments is 1–10 μm (Le Guehennec et al. 2007) and is related to the interlocking between the dental implant surface and the bone. The surfaces with nano-sized roughness influence the osseointegration rate by adsorbing proteins and increasing the adhesion of the osteoblastic cells (Brett et al. 2004). Depending on the type of measurements and techniques used, the range of optimal surface roughness contributed to osseointegration varies considerably from 1

Date:
Accepted 15 July 2011

To cite this article:
Lee S-Y, Yang D-J, Yeo S, An H-W, Ryoo KH, Park K-B. The cytocompatibility and osseointegration of the Ti implants with XPEED® surfaces.
Clin. Oral Impl. Res. **00,** 2011, 1–7
doi: 10.1111/j.1600-0501.2011.02304.x

to 23 μm (Buser et al. 1991, 1999; Wong et al. 1995; Wennerberg & Albrektsson 2000; Grassi et al. 2006; Shibli et al. 2007).

With the surface roughness and topography, the surface chemistry plays an important role for osseointegration. Titanium (Ti) and Ti alloys are bioinert surfaces and are not able to directly bond with bone. One of the methods of increasing surface reactivity is coating the Ti surface with layers of calcium phosphate. Plasma-sprayed HA coating is a widely used method. The studies reported that the dental implants with the HA coating enhance osseointegration as compared to non-coated dental implants (Geurs et al. 2002; Barrere et al. 2003). Another study reported that the survival rate of the dental implant with or without the HA coating is similar (Lee et al. 2000) or decreases in the dental implants with the HA coating (Wheeler 1996). Plasma-sprayed HA coating produces the bioactive implant surface but has several disadvantages. The plasma coating is closely attached to the bone tissue and is delaminated from the surface Ti implant (Hanisch et al. 1997; Albrektsson 1998). Another method of increasing surface reactivity is to coat the nanostructured calcium into the Ti surface. The nanostructured calcium coating reported a large degree of effectiveness in many *in vitro* and *in vivo* studies. The *in vitro* studies have reported that surface modification from the use of calcium ions increased the growth of osteoblastic cells and promoted the precipitation of apatite on the Ti surfaces in simulated body fluid (Hamad et al. 2002; Nayab et al. 2004, 2005; Park et al. 2007). Also the effects of cell adhesion on calcium incorporated into the Ti surface was reduced in human alveolar bone cells (Nayab et al. 2004) and MG-63 cells (Nayab et al. 2005) and increased in human osteoblasts (Webster et al. 2003). Several *in vivo* studies have reported that incorporating calcium into Ti implants by hydrothermal treatment stimulated osseointegration by increasing BIC% more than in untreated Ti implants in rabbit models (Park et al. 2007, 2008; Park et al. 2009). It was reported that the surface roughness was modified only at the nano-scale level but not at the micron-scale level after Ca incorporation by hydrothermal modification (Park et al. 2007, 2008). Although several studies have documented the osteoblast response in cell proliferation and cell attachment on disks with incorporated calcium, few have investigated the effects of calcium ions on the three dimensional cellular environment.

We aimed to investigate the cell proliferation on and cell attachment to the Ti implants with nanostructured calcium coating (XPEED® surfaces). In previous studies, the amount of calcium ions released from the Ti implants with calcium incorporation was not measured. We measured the amount of calcium ions released from the Ti implants with XPEED® surfaces. Instead of Hank's Balanced Salt Solution (HBSS), our studies on apatite-forming ability used a modified-simulated body fluid (m-SBF). Also, Ti implants were used instead of square or disk specimens. In addition, we investigated the apatite formation on different parts of the Ti implants, such as the crest, root portion, and cutting edge. The previous studies evaluated the osseointegration of the Ti implants produced by grit-blasting/acid-etching techniques and the Ti6Al4V alloy implants by grit-blasting with the addition of calcium ions (Park et al. 2007, 2009). We investigated the osseointegration using removal torque tests in rabbit tibiae and by histomorphometric analysis in rabbit femurs on grit-blasted Ti implants with XPEED® surfaces.

Material and methods

Implant design

Commercial Ti implants (EZ Plus™ Internal implants) roughened by grit-blasting were used in this study (Megagen Co. Ltd., Kyungsan, Korea). The Ti implants had a thread diameter of 4.0 mm and a length of 10 mm, except for those used in the animal study. For the animal study, the implant thread diameter was 3.3 mm and the length of the implant was 5.0 mm. The calcium-incorporated Ti implants, that is, the Ti implants with XPEED® surfaces, were prepared by hydrothermal reaction in the same manner as previous studies (Park et al. 2007, 2008; Suh et al. 2007). Briefly, Ti implants were hydrothermally treated in a mixed solution containing 2 mM CaO and 0.2 M NaOH at 180°C for 2 h. Then, the Ti implants with XPEED® surfaces were rinsed and dried. All implants used this study were sterilized by γ-irradiation.

Surface characterization

The morphology of the Ti implant surface was observed by scanning electron microscope (SEM) equipped with energy dispersive X-spectroscope (SEM/EDS, S-4800, Hitachi, Tokyo, Japan). The surface roughness was evaluated by a surface roughness measuring system (Form Talysurf Series 2, Taylor Hobson, Leicester, England). Two Ti implants from each group were used and the surface roughness was measured on the same Ti implant three times. The measurement point of surface roughness was the lateral flat side of the lower part of the implant, namely the cutting edge.

Released amount of calcium

Implants ($n = 3$) were incubated at 37°C in 5 ml of the saline for 2, 4, and 8 weeks. After incubation period, the solution was harvested from the implants. The concentration of calcium ions from the harvested solution was analyzed by an inductively coupled plasma optical emission spectrometer (ICP-OES; Optima 7300DV, Perkin Elmer, Shelton, CT, USA).

Evaluation of apatite-forming ability

Implants were immersed at 37°C in 25 ml of the m-SBF for 3 weeks. The lower part of the implants was located toward the bottom of the bottle. The m-SBF was prepared as follows (Oyane et al. 2003). First, each reagent in the sequence listed in Table 1 was completely dissolved in distilled water. It was buffered using 2-(4-(2-hydroxyethyl)-1-piperazinyl) ethanesulfonic acid (HEPES) and NaOH at pH 7.4. The solution was changed twice a week. After 13 days, the implant was washed with distilled water and then dried for 24 h. The apatite was examined using a SEM equipped with an energy dispersive X-spectroscope (SEM/EDS, S-4800, Hitachi).

Cell proliferation

The MC3T3-E1 cells (5×10^5 cells), a mouse calvaria-derived osteoblast-like cell line, and implants in α-modified Eagle's medium (α-MEM) were repeatedly rotated by using a rotation plate (2 rpm) in a flat-bottom tube for 3 h at 37°C (van den Dolder et al. 2002). The cells attached to the implants were incu-

Table 1. **Order, reagent, purity, and amount for preparation of m-SBF**

Order	Reagent	Purity (%)	Amount (g)
1	NaCl	>99.5	5.403
2	$NaHCO_3$	>99.5	0.504
3	Na_2CO_3	>99.5	0.426
4	KCl	>99.5	0.225
5	$K_2HPO_43H_20$	>99.0	0.230
6	$MgCl_2$–$6H_2O$	>98.0	0.311
7	HEPES*	>99.9	17.892
8	$CaCl_2$	>95.0	0.293
9	Na_2S0_4	>99.0	0.072
10	1.0 M NaOH	–	≒15ml

*HEPES was previously dissolved in 100 ml of 0.2 M NaOH.

bated at 37°C in a humidified atmosphere of 5% CO_2 for 3, 5, and 7 days. MTT (3-(4,5-dimethylthiazol-2yl)-2,5-diphenyl tetrazolium bromide) assay was performed for the cell proliferation at the indicated time. A quantity of 0.5 mg/ml of MTT solution was added to each well. After 3 h, the MTT solution was aspirated and the dimethylsulfoxide was added to solubilize the formed formazan. The optical density was measured at a wavelength of 570 nm using an ELISA reader (Power-Wave XS, Bio-Tek, Winooski, VT, USA).

Cell attachment

The MC3T3-E1 cells (5×10^5 cells) and implants in α-MEM were repeatedly rotated by using a rotation plate (2 rpm) in a flat-bottomed tube for 3 h at 37°C. The cells attached to implants were incubated at 37°C in a humidified atmosphere of 5% CO_2 for 10 days. After incubation, the implants were washed twice with phosphate buffered saline (pH 7.4). Fixation was carried out for 30 min in 2% glutaraldehyde. The implants were then washed twice with 0.1 M sodium cacodylate buffer (pH 7.4), dehydrated sequentially in 25%, 50%, 75%, 95%, and 100% ethanol, for 5 min each, and dried with tetramethylsilane. The specimens were coated with gold, examined, and photographed using a SEM equipped with an energy dispersive X-spectroscope (SEM/EDS, S-4800, Hitachi).

Animals and surgical procedure

The animal experiment was approved by the Institutional Animal Care and Use Committee of Yeungnam National University Hospital, Daegu, Korea. Ten adult male 20-week-old New Zealand White Rabbits weighing 3.5–4 kg were used. The surgical sites were the flat medial surfaces of the femoral condyles for the histomorphometric analysis and the medial surfaces of the proximal tibiae for the removal torque test. The surgical regions were shaved and the skin was disinfected with iodine and hexamidine. General anesthesia was performed by the intramuscular injection of a mixture of 1.3 ml of 100 mg/ml ketamin (Yuhan, Seoul, Korea) and 0.2 ml of Rumpun (7 mg/kg; Bayer Korea, Seoul, Korea) and the local anesthetic was 1 ml of 2% lidocaine (Yuhan). The incision for the surgical sites was made on the medial surface of the distal femur and the medial surface of the proximal tibiae from the skin to the periosteum. The osteotomy was performed according to the recommended surgical protocol supplied by the manufacturer. The holes for implant implantation were drilled in sequential order. A set of three control implants (implants with RBM surfaces) and a set of three experimental implants (implants with XPEED® surfaces) were randomly placed in the right legs and left legs (two implants in the tibia and one implant in the femur). The implants with resorbable blast media (RBM) surfaces ($n = 30$) and the implants with XPEED® surfaces ($n = 30$) were implanted with the recommended torque. All implants were inserted up to the bone cortex. The surgical site was then sutured with Vicryl (Ethicon, Somerville, NJ, USA), and the antibiotic Baytril (Bayer Korea) and analgesic Nobin (Bayer Korea) were injected intramuscularly to minimize infection and pain.

Removal torque tests

After 4 weeks, to evaluate implant stability, removal torque tests were performed in the proximal tibia bed with the implants. After the incision of the surgical site, the fixture mount was connected. The legs of the rabbit were stabilized by a collet chuck and a digital torque meter (Mark-10, New York, USA) was fixed by using the test standard (Mark-10). The removal torque was measured by using a digital torque meter positioned in the same direction of the implant axis with constant speed.

Histomorphometric evaluation

After 4 weeks, tissues containing implants from the femoral condyles for histomorphometric evaluation were harvested and fixed in 70% ethanol. The tissue was dehydrated sequentially in ethanol, and then embedded in methyl methacrylate resin. The sections of 20 μm thickness containing the central regions of the implants were produced by a Macrocutting and grinding system (Exakt 310 CP series, Exakt Apparatebau, Norderstedt, Germany). The sections were stained with Villanueva staining and were photographed with a trinocular microscope (CX31; Olympus, Tokyo, Japan). The percentage of bone-to-implant contact (BIC%) and the percentage of bone area (bone area%) were measured over all threads. BIC% was measured as a percentage of the length of mineralized bone contacting the implant surface directly and bone area% was evaluated by measuring the amount of mineralized bone inside all threads. The percentage of bone-to-implant contact (BIC%) and the percentage of bone area was measured with an image analysis program (Analysis TS Auto; Olympus).

Statistical analysis

Statistical analysis was performed using SPSS 11.0 statistical system (SPSS Inc., Chicago, IL, USA). One-way analysis of variance with Tukey's multiple comparisons test was performed to evaluate differences in released amount of calcium and cell proliferation between groups. The paired Student *t*-test was performed to compare the significance of the differences in surface roughness, removal torque, BIC%, and bone area%. Values of P were statistically significant at <0.05.

Results

Surface characteristics

The surface topography of the Ti implants was observed (Fig. 1). The surface morphology of the Ti implants with RBM surfaces caused by grit-blasting showed the micro-rough surface topography and the irregular indentation. By incorporating calcium ions, the Ti implants with XPEED® surfaces were observed to have a similar surface morphol-

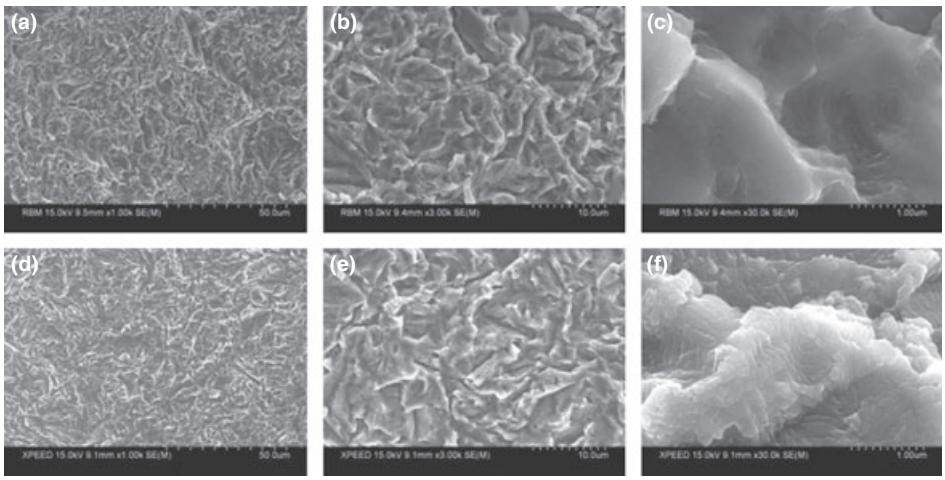

Fig. 1. Scanning electron microscope image of the Ti implants with RBM surfaces (a, b, c) and the Ti implants with XPEED® surfaces (d, e, f) at magnifications of ×1000 (a, d), ×3000 (b, e), and ×30,000 (c, f).

Table 2. **Surface roughness parameters of Ti implants (mean ± SD; *n* = 6)**

Surface treatment	R_a (μm)	R_q (μm)	R_t (μm)	R_{ZDIN} (μm)
RBM	1.56 ± 0.08	2.11 ± 0.13	18.53 ± 1.56	12.55 ± 0.32
XPEED	1.63 ± 0.22	2.16 ± 0.30	15.76 ± 0.29*	12.46:1:0.55

R_a, the arithmetic average of the absolute height values of all points of the profile; R_q, the root mean square of the values of all points of fhe profile; *R*t, the maximum peak-to-valley height of the entire measurement trace; R_{ZDIN}, the arithmetic average of the maxinum peak-to-valley height of the roughness values of five consecutive sampling sections over the filtered profile.
*Significant differences between the Ti implants with RBM surfaces and the Ti implants with XPEED surfaces at $P = 0.02$.

ogy to that of the Ti implants with RBM surfaces at lower magnifications (×1000, ×3000). At the higher magnification (×30,000), Ti implants with XPEED® surfaces were observed to have a surface nanostructure with a regular shape. The average surface roughness (Ra) of the Ti implants with RBM surfaces and XPEED® surfaces was similar (Table 2) ($P > 0.1$).

Apatite formation

After the Ti implants had been incubated in m-SBF for the indicated time, the Ti implants with the XPEED® surfaces had formed more apatite than the Ti implants with RBM surfaces (Fig. 2). Interestingly, the apatite formation was observed on all surfaces containing the root, crest portion, and cutting edge of the Ti implants with XPEED® surfaces but the Ti implants with RBM surfaces showed only apatite formation at the crest portion of the Ti implants with RBM surfaces, but not at the root portion and at the cutting edge.

Release of calcium

After the Ti implants had been immersed in the physiological saline solution for the indicated time, the calcium ions released from the Ti implants with XPEED® surfaces increased with longer incubation times ($P < 0.001$) but did not increase in the Ti implants with RBM surfaces ($P > 0.05$) (Table 3).

Cell proliferation

The cell proliferation in the Ti implants was analyzed by MTT assay in mouse osteoblastic cells (MC3T3-E1 cells). The data were expressed as a percentage of the Ti implants with RBM surfaces at 3 days. The Ti implants with XPEED® surfaces showed similar absorbance with that of cells on the Ti implants with RBM surfaces for the incubated time (Fig. 3). There was no statistical difference in cell proliferation between the Ti implants with RBM surfaces and the Ti implants with XPEED® surfaces ($P > 0.1$).

Cell attachment

At 10 days after seeding, the cells were evenly attached to the surfaces of both the Ti implants with RBM surfaces and the Ti implants with XPEED® surfaces (Fig. 4).

Removal torque testing

The mean removal torque of the Ti implants with XPEED® surfaces was 33.3 ± 4.1 Ncm and that of the Ti implants with RBM surfaces was 23.7 ± 8.3 Ncm. The mean removal torque of the Ti implants with XPEED® surfaces was even higher than that of the Ti implants with RBM surfaces ($P = 0.038$).

Histological evaluation

At 4 weeks after implantation, direct bone contact was observed along the surface of all Ti implants (Fig. 5). There was no histological inflammation at the bone-implant boundary (Fig. 5). The mean BIC% in all threads was 30.7 ± 2.4% for the Ti implants with RBM surfaces and 35.8 ± 1.7% for the Ti implants with XPEED® surfaces (Fig. 6). The mean bone area% was 35.1 ± 1.3% for the Ti implants with RBM surfaces and 37.1 ± 3.0% for the Ti implants with XPEED® surfaces (Fig. 6). The BIC% of the Ti implants with XPEED® surfaces was enhanced compared to the Ti implants with RBM surfaces ($P = 0.03$). However, the Ti implants with XPEED® surfaces showed no significant enhancement in the mean bone area% ($P > 0.1$).

Discussion

In this study, Ti implants with XPEED® surfaces produced by hydrothermal treatment formed more apatite than the Ti implants with RBM surfaces when incubated in modified-simulated body fluid (m-SBF) for the same period. Simulated body fluid (SBF) is a fluid with ion concentrations similar to that of human blood plasma. SBF is used to evaluate the *in vitro* apatite-forming ability of the surface of materials, and this ability is consistent with the *in vivo* bone-bonding ability. The artificial materials used for the biomimetic production of bone-like apatite were

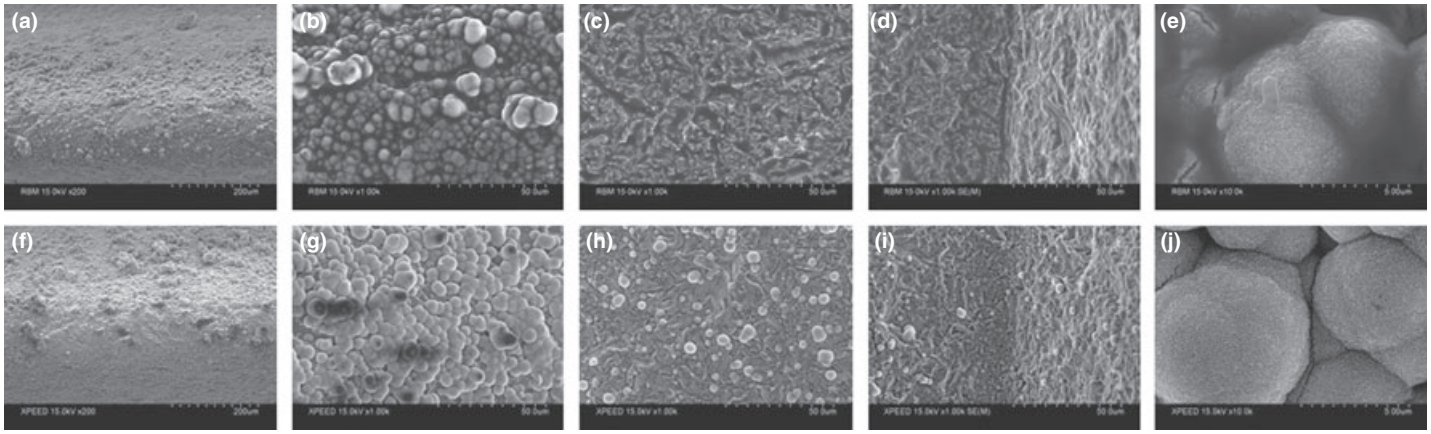

Fig. 2. Scanning electron microscope images of the Ti implants with RBM surfaces (a, b, c, d, e) and the Ti implants with XPEED® surfaces (f, g, h, i, j) incubated in m-SBF for 13 days. (a, b, e, f, g, j) Crest portion, (c, h) root portion, and (d, i) cutting edge of Ti implants at magnifications of ×200 (a, f), ×1000 (b, c, d, g, h, i), and ×10,000 (e, j). Ti implants with XPEED® surfaces showed more apatite formation over the surface than the other implants.

Table 3. **Release of calcium ions from Ti implants with XPEED® surfaces (mean ± SD; *n* = 3)**

	Immersion line (weeks)	Concentration (ppm)
RBM	2	0.77 ± 0.02
	4	0.79 ± 0.02
	8	0.78 ± 0.01
XPEED	2	1.22 ± 0.01*
	4	1.47 ± 0.01*, †
	8	1.77 ± 0.01*,†

*Significant differences compared to Hie Ti implants with RBM surfaces and with XPEED surfaces at the same time ($P < 0.05$).
†Significant differences between 2 and 4 weeks or 4 and 8 weeks within the Ti Implants with XPEED surfaces ($P < 0.05$).

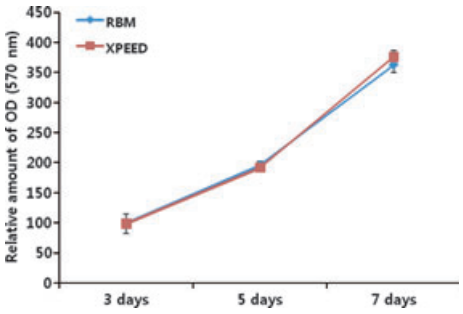

Fig. 3. Cell proliferation of the Ti implants with RBM surfaces and the Ti implants with XPEED® surfaces for 3, 5, and 7 days. Data are expressed as the mean ± SD ($n = 3$). There were not significant differences between the Ti implants with RBM surfaces and the Ti implants with XPEED® surfaces; $P > 0.1$.

conventional SBF (c-SBF), revised SBF (r-SBF), m-SBF, and HBSS. Several studies have reported that calcium-incorporated square specimens formed more apatite than untreated specimens (Park et al. 2007, 2008). These studies used HBSS among artificial materials for its apatite-forming ability. However, we used m-SBF, which has an ion concentration nearly equal to that of blood plasma and its ion concentration remains nearly unchanged during its storage period (Oyane et al. 2003). Among artificial materials designed for their apatite-forming ability, the use of both the Ti implants and m-SBF mimics the conditions of the biological environment much better, comparitively, than do square Ti specimens and HBSS . Our studies showed that there was no apatite formed at the root portion and the cutting edge of the Ti implants with RBM surfaces but formed apatite at the Ti implants with XPEED® surfaces for the same period. This means that it takes more time for the apatite to form at the root portion and the cutting edge of Ti implants than the crest portion of Ti implants. The time required for the apatite formation at the root portion and cutting edge of the Ti implants with RBM surfaces were decreased by incorporating calcium ions into the surface of the Ti implants.

The square Ti and Ti6Al4V specimens with the incorporation of calcium ions increased significantly the proliferation of MC3T3-E1 preosteoblast as compared with those of the microroughened surfaces (Park et al. 2007, 2008). The polished Ti disks implanted with calcium ions enhanced the proliferation of alveolar bone cells and MG-63 cells (Nayab et al. 2004). However, our studies demonstrated that the Ti implants with XPEED® surfaces and the Ti implants with RBM surfaces showed a similar proliferation rate for 3, 5, and 7 days. This fact is due to the difference in the type of specimens

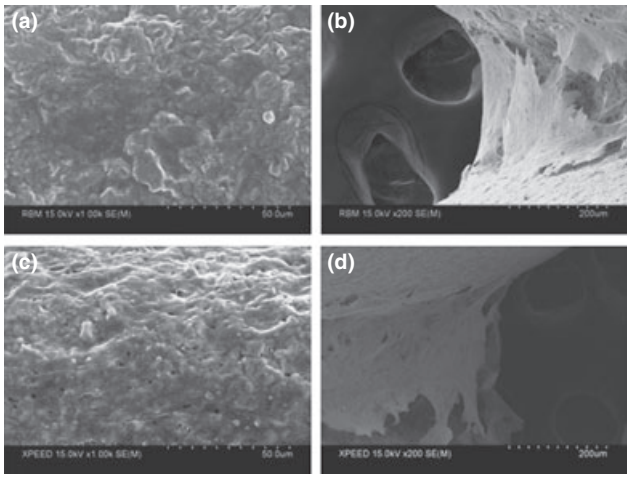

Fig. 4. Scanning electron microscope images of MC3T3-E1 cells incubated on the Ti implants with RBM surfaces (a, b) and the Ti implants with XPEED® surfaces (c, d) at magnifications of ×1000 (a, c) and ×200 (b, d). Cells were evenly attached on the surface of both the Ti implants with RBM surfaces and the Ti implants with XPEED® surfaces.

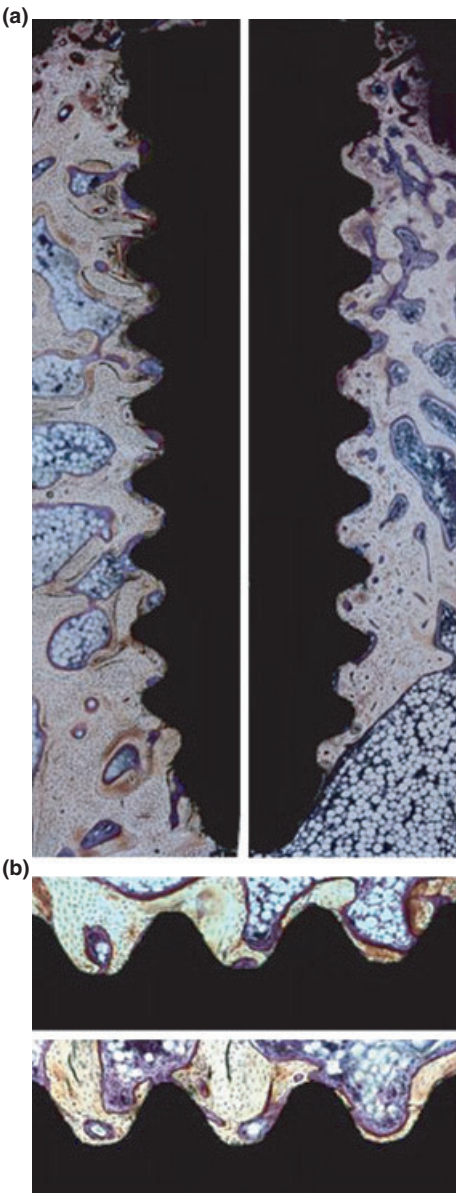

Fig. 5. Histological sections of the Ti implants with RBM surfaces (left) and the Ti implants with XPEED surfaces (right) in all threads (a) and the Ti implants with RBM surfaces (upper) and the Ti implants with XPEED® surfaces (lower) in three threads of implants (b) 4 weeks after implantation in rabbit femurs. Magnification of ×40 (a) and ×100 (b) (stained with Villaneueva stain). Direct bone contact can be observed along the surface of both Ti implants.

(disk versus fixture), raw materials, type of surface treatments, and type of cells. The release of calcium ions from the surface of the Ti implants may take a much longer time than the surface of the Ti disk specimens. Our data indicated that the amount of calcium ions released until 7 days was very little in the cell culture media (Table 3). The amount of calcium ions released was probably not sufficient to affect cell proliferation. Our studies also showed that cells were

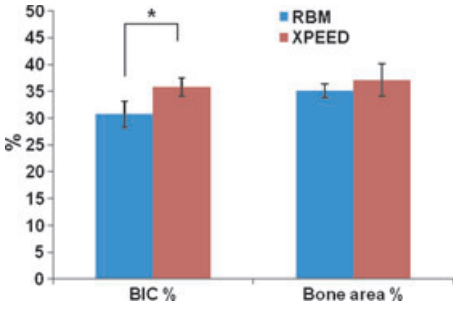

Fig. 6. Mean percentage of the bone-to-implant contact (BIC%) and bone area in all threads of Ti implants at 4 weeks after implantation in rabbit femurs. The BIC% was enhanced slightly in the Ti implants with XPEED® surfaces (35.8 ± 1.7%) compared with the Ti implants with RBM surfaces (30.7 ± 2.4%). No significant enhancement was observed in the percentage of the bone area between the Ti implants with RBM surfaces (37.1 ± 1.3%) and the Ti implant with XPEED® surfaces (39.5 ± 3.0%). (*$P < 0.05$).

attached over the entire surface on both Ti implants. These studies are significant because cell adhesion and cell distribution on the Ti implants could be observed unlike the previous studies that used incorporated Ti disks (Nayab et al. 2004, 2005).

Our studies showed that the BIC% of the Ti implants with RBM surfaces was 30.7 ± 2.4% at 4 weeks after implantation in all threads of implants, and the Ti implants with XPEED® surfaces increased slightly the BIC% to 35.8 ± 1.7%. In addition, our results increased only the BIC% but not the bone area%. The increased BIC% is related to the osseointegration in agreement with several studies reporting a direct correlation between BIC% and osseointegration, but the bone area% is not related to the osseointegration (Morra et al. 2006; Park et al. 2009). These findings support the results of previous studies reporting great osseointegration of calcium incorporation (Park et al. 2007, 2009; Suh et al. 2007). Our studies indicated that the R_a (average surface roughness) of the Ti implants with XPEED® surfaces was similar to that of the Ti implants with RBM surfaces but the R_t (the maximum peak-to-valley height of the entire measurement trace) of the Ti implants with XPEED® surfaces decreased slightly compared to that of the Ti implants with RBM surfaces ($P = 0.02$). The incorporation of nanostructured calcium seems to induce a subtle change in microtopography as shown in a little reduction of R_t. We assume that the micro-structured surface effectively cannot contribute osseointegration. It seems that the nanostructure of the surface produced by the incorporation of calcium ions as well as the calcium ions themselves contribute to enhanced osseointegration of micro-structured Ti implants by stimulating osteoblastic differentiation (Park et al. 2008) and apatite formation (Park et al. 2007, 2008) by the adsorption of phosphate ions due to the attractive force of the electric charge (Hanawa et al. 1998). The calcium incorporated into the microstructured Ti surface increased the expression of osteoblastic genes such as alkaline phosphate (ALP), osteopontin, and osteocalcin (OC) in MC3T3-E1 cells (Park et al. 2008). We have showed that the amount of calcium ions released from the Ti implants with XPEED® surfaces increased with longer incubation times. The amount of calcium ions released from the surface of the Ti implants was not analyzed in previous studies. Released calcium ions may stimulate the proliferation of mesenchymal cells mediated by G protein-coupled receptors between surrounding bone and the Ti implants with XPEED® surfaces (Mailland et al. 1997). Further detailed studies are needed to confirm the effects of calcium ions incorporated into Ti implants on the osteoblastic differentiation and osseointegration in clinical studies. We continue to research clinical applications to better understand the effects of Ti implants with XPEED® surfaces in areas of poor quality bone such as in the posterior maxilla.

This study suggests that the micro-roughened Ti implants with XPEED® surfaces maintain cell attachment and proliferation and the calcium ions incorporated into the Ti implant surfaces enhance the *in vitro* apatite formation, removal of torque value, and osseointegration. Ti implants with XPEED® surfaces may induce strong bone integration by improving osseointegration of grit-blasted Ti implants. The XPEED surface treatment of Ti dental implants may be an effective method for rapid osseointegration in areas of poor quality bone.

References

Albrektsson, T. (1998) Hydroxyapatite-coated implants: a case against their use. *Journal of Oral and Maxillofacial Surgery* **56**: 1312–1326.

Barrere, F., van der Valk, C.M., Meijer, G., Dalmeijer, R.A., de Groot, K. & Layrolle, P. (2003) Osteointegration of biomimetic apatite coating applied onto dense and porous metal implants in femurs of goats. *Journal of Biomedical Materials Research Part B: Applied Biomaterials* **67**: 655–665.

Brett, P.M., Harle, J., Salih, V., Mihoc, R., Olsen, I., Jones, F.H. & Tonetti, M. (2004) Roughness response genes in osteoblasts. *Bone* **35**: 124–133.

Buser, D., Nydegger, T., Oxland, T., Cochran, D.L., Schenk, R.K., Hirt, H.P., Snetivy, D. & Nolte, L. P. (1999) Interface shear strength of titanium implants with a sandblasted and acid-etched surface: a biomechanical study in the maxilla of miniature pigs. *Journal of Biomedical Materials Research* **45**: 75–83.

Buser, D., Schenk, R.K., Steinemann, S., Fiorellini, J.P., Fox, C.H. & Stich, H. (1991) Influence of surface characteristics on bone integration of titanium implants. A histomorphometric study in miniature pigs. *Journal of Biomedical Materials Research* **25**: 889–902.

van den Dolder, J., Vehof, J.W., Spauwen, P.H. & Jansen, J.A. (2002) Bone formation by rat bone marrow cells cultured on titanium fiber mesh: effect of *in vitro* culture time. *Journal of Biomedical Materials Research* **62**: 350–358.

Geurs, N.C., Jeffcoat, R.L., McGlumphy, E.A., Reddy, M.S. & Jeffcoat, M.K. (2002) Influence of implant geometry and surface characteristics on progressive osseointegration. *The International Journal of Oral and Maxillofacial Implants* **17**: 811–815.

Gotfredsen, K., Wennerberg, A., Johansson, C., Skovgaard, L.T. & Hjorting-Hansen, E. (1995) Anchorage of TiO2-blasted, HA-coated, and machined implants: an experimental study with rabbits. *Journal of Biomedical Materials Research* **29**: 1223–1231.

Grassi, S., Piattelli, A., de Figueiredo, L.C., Feres, M., de Melo, L., Iezzi, G., Alba, R.C. Jr & Shibli, J.A. (2006) Histologic evaluation of early human bone response to different implant surfaces. *Journal of Periodontology* **77**: 1736–1743.

Hamad, K., Kon, M., Hanawa, T., Yokoyama, K., Miyamoto, Y. & Asaoka, K. (2002) Hydrothermal modification of titanium surface in calcium solutions. *Biomaterials* **23**: 2265–2272.

Hanawa, T., Kon, M., Doi, H., Ukai, H., Murakami, K., Hamanaka, H. & Asaoka, K. (1998) Amount of hydroxyl radical on calcium-ion-implanted titanium and point of zero charge of constituent oxide of the surface-modified layer. *Journal of Materials Science: Materials in Medicine* **9**: 89–92.

Hanisch, O., Cortella, C.A., Boskovic, M.M., James, R.A., Slots, J. & Wikesjö, U.M. (1997) Experimental peri-implant tissue breakdown around hydroxyapatite-coated implants. *Journal of Periodontology* **68**: 59–66.

Le Guehennec, L., Soueidan, A., Layrolle, P. & Amouriq, Y. (2007) Surface treatments of titanium dental implants for rapid osseointegration. *Dental Materials* **23**: 844–854.

Lee, J.J., Rouhfar, L. & Beirne, O.R., (2000) Survival of hydroxyapatite-coated implants: a meta-analytic review. *Journal of Oral and Maxillofacial Surgery* **58**: 1372–1379; discussion 1379-1380.

Mailland, M., Waelchli, R., Ruat, M., Boddeke, H. G. & Seuwen, K. (1997) Stimulation of cell proliferation by calcium and a calcimimetic compound. *Endocrinology* **138**: 3601–3605.

Morra, M., Cassinelli, C., Cascardo, G., Mazzucco, L., Borzini, P., Fini, M., Giavaresi, G. & Giardino, R. (2006) Collagen I-coated titanium surfaces: mesenchymal cell adhesion and *in vivo* evaluation in trabecular bone implants. *Journal of Biomedical Materials Research Part A* **78**: 449–458.

Nayab, S.N., Jones, F.H. & Olsen, I. (2004) Human alveolar bone cell adhesion and growth on ion-implanted titanium. *Journal of Biomedical Materials Research Part A* **69**: 651–657.

Nayab, S.N., Jones, F.H. & Olsen, I. (2005) Effects of calcium ion implantation on human bone cell interaction with titanium. *Biomaterials* **26**: 4717–4727.

Oyane, A., Kim, H.M., Furuya, T., Kokubo, T., Miyazaki, T. & Nakamura, T. (2003) Preparation and assessment of revised simulated body fluids. *Journal of Biomedical Materials Research Part A* **65**: 188–195.

Park, J.W., Kim, H.K., Kim, Y.J., An, C.H. & Hanawa, T. (2009) Enhanced osteoconductivity of micro-structured titanium implants (XiVE S CELLplus™) by addition of surface calcium chemistry: a histomorphometric study in the rabbit femur. *Clinical Oral Implants Research* **20**: 684–690.

Park, J.W., Park, K.B. & Suh, J.Y. (2007) Effects of calcium ion incorporation on bone healing of Ti6Al4V alloy implants in rabbit tibiae. *Biomaterials* **28**: 3306–3313.

Park, J.W., Suh, J.Y. & Chung, H.J. (2008) Effects of calcium ion incorporation on osteoblast gene expression in MC3T3-E1 cells cultured on micro-structured titanium surfaces. *Journal of Biomedical Materials Research* **86**: 117–126.

Shibli, J.A., Grassi, S., de Figueiredo, L.C., Feres, M., Marcantonio, E. Jr, Iezzi, G. & Piattelli, A. (2007) Influence of implant surface topography on early osseointegration: a histological study in human jaws. *Journal of Biomedical Materials Research Part B: Applied Biomaterials* **80**: 377–385.

Suh, J.Y., Jeung, O.C., Choi, B.J. & Park, J.W. (2007) Effects of a novel calcium titanate coating on the osseointegration of blasted endosseous implants in rabbit tibiae. *Clinical Oral Implants Research* **18**: 362–369.

Webster, T.J., Ergun, C., Doremus, R.H. & Lanford, W.A. (2003) Increased osteoblast adhesion on titanium-coated hydroxylapatite that forms CaTiO3. *Journal of Biomedical Materials Research Part A* **67**: 975–980.

Wennerberg, A. & Albrektsson, T. (2000) Suggested guidelines for the topographic evaluation of implant surfaces. *The International Journal of Oral and Maxillofacial Implants* **15**: 331–344.

Wennerberg, A., Albrektsson, T., Andersson, B. & Krol, J.J. (1995) A histomorphometric and removal torque study of screw-shaped titanium implants with three different surface topographies. *Clinical Oral Implants Research* **6**: 24–30.

Wheeler, S.L. (1996) Eight-year clinical retrospective study of titanium plasma-sprayed and hydroxyapatite-coated cylinder implants. *The International Journal of Oral and Maxillofacial Implants* **11**: 340–350.

Wong, M., Eulenberger, J., Schenk, R. & Hunziker, E. (1995) Effect of surface topology on the osseointegration of implant materials in trabecular bone. *Journal of Biomedical Materials Research* **29**: 1567–1575.